3D Numerical modelling of residual stresses induced in finish turning of a fillet radius on a shaft made of 15-5PH

Maxime Dumas, Dorian Fabre, Frédéric Valiorgue, Guillaume Kermouche, Bertrand Truffart, Mathieu Girinon, Alexandre Brosse, Habib Karaouni, Joël Rech

Available online at www.sciencedirect.com

ScienceDirect

Procedia CIRP 117 (2023) 122–127

www.elsevier.com/locate/procedia

19th CIRP Conference on Modeling of Machining Operations

3D Numerical modelling of residual stresses induced in finish turning of a fillet radius on a shaft made of 15-5PH

Maxime DUMAS[a,c], Dorian FABRE[a], Frédéric VALIORGUE[a], Guillaume KERMOUCHE[b], Bertrand TRUFFART[c], Mathieu GIRINON[d], Alexandre BROSSE[e], Habib KARAOUNI[f], Joel RECH[a,*]

[a] *Ecole Centrale de Lyon – ENISE, LTDS UMR CNRS 5513, 58 Rue Jean Parot, 42100*
[b] *Ecole des Mines de Saint Etienne, Centre SMS, Laboratoire LGF UMR 5307, 158 Cours Fauriel, 42023 Saint Etienne, France*
[c] *Airbus Helicopters, LMP, Aéroport Marseille Provence, 13725 Marignane*
[d] *Cetim, 7 rue de la Presse, 42952 Saint-Etienne*
[e] *Framatome, 10 rue Juliette Récamier, 69456 Lyon*
[e] *SAFRAN Tech, Rue des Jeunes-Bois, 78772 Magnye-les-Hameaux*

* Corresponding author. Tel.: +33477438484. *E-mail address:* joel.rech@enise.fr

Abstract

The objective of this paper is to model the residual stress generation mechanisms induced during the finish turning of a fillet radius on a 15-5PH steel shaft. The model, based on the 3D thermo-mechanical equivalent loading method, is used to predict the continuous variation of residual stresses resulting from the continuous variation of the machined sections in the fillet radius. Finally, experimental tests are carried out to compare the numerical results with the residual stress measurements made by X-ray diffraction in some positions.

Keywords: Turning ; Concave radius ; residual stresses ; numerical modeling

1. Introduction

Mechanical industries have to ensure the fatigue life of their safety engineering components. Fatigue resistance is directly influenced by several parameters such as surface roughness, residual stress and microstructure, which are commonly summarized by the term ”surface integrity” [1]. The influence of surface integrity on the functional performance and life of machined components has been widely discussed in the literature [2]. For example, [3] have reported the significant role that residual stresses play in determining the fatigue life of critical products. The residual stress state depends on the thermo-mechanical loadings induced by all the previous manufacturing operations (heat treatment, forming, rough machining…), even if the last operation has a major responsibility [4]. This paper focuses on finishing turning operations as they are among the most widely used finishing operations for shafts. A recent paper [5] has proposed an original 3D numerical model to predict rapidly and accurately the residual stress state induced in longitudinal finish turning. On the contrary to the wide majority of previous models [6,7] that considers the whole cutting process (chip+tool+part), this recent model [5] consists in modelling the residual stress generation by removing the chip formation and cutting tool and replacing it with 3D equivalent thermo-mechanical loadings. Figure 1 illustrates its key steps. As shown in Figure 1-1, it is first necessary to define the cut section CS. Its geometry is defined by the cutting tool geometry (edge radius, lead angle, ...) and the cutting conditions (depth of cut a_p, feed f).

2212-8271
10.1016/j.procir.2023.03.022

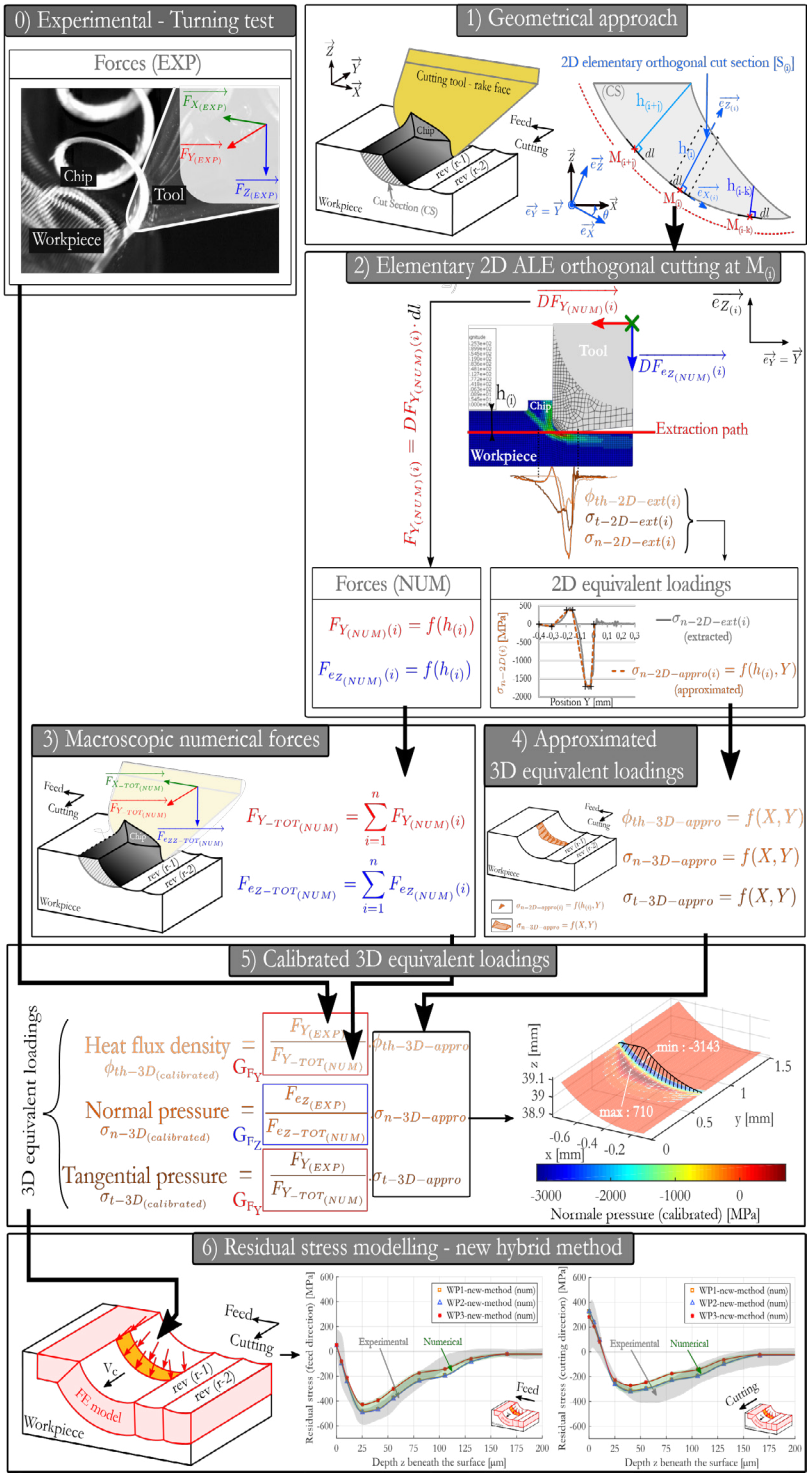

Fig. 1. Principle of the 3D equivalent thermo-mechanical loadings model [5].

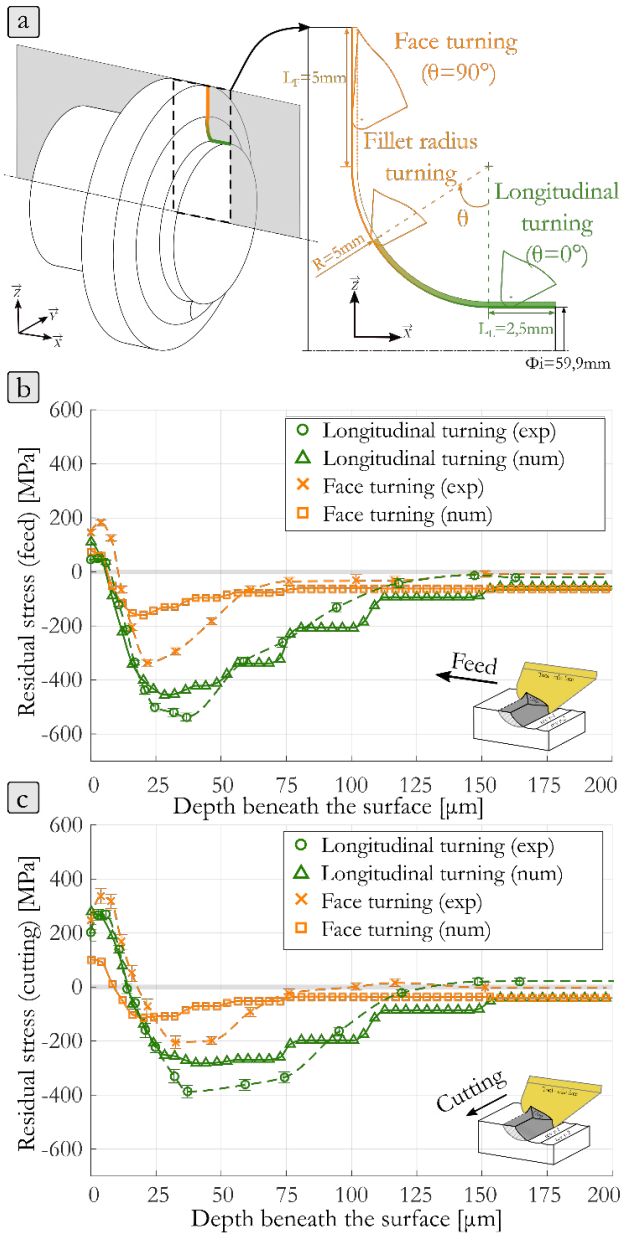

Fig. 2. Influence of the radial position on residual stresses induced by turning.

The cut section CS is divided into several 2D elementary orthogonal sections $S_{(i)}$ having a local uncut chip thickness $h_{(i)}$ (Figure 1-1). For each section $S_{(i)}$, a 2D numerical model (ABAQUS explicit with an ALE formulation) simulates the material removal as shown in Figure 1-2. Based on these simulations, the thermo-mechanical loadings induced on the future machined surface of each section $S_{(i)}$ are extracted along the line called "extraction path". This provides the 2D density of heat flux $\varphi_{th-2D(i)}$, the normal stress $\sigma_{n-2D(i)}$ and the tangential stress $\sigma_{t-2D(i)}$ along the extraction path, applied to the workpiece (Figure 1-2). By combining these 2D loadings on the effective machined surface (a cylindrical groove in this case study – Figure 1-4), it becomes possible to model the 3D density of heat flux $\varphi_{th-3D-appro}$, normal stress $\sigma_{n-3D-appro}$ and tangential stress $\sigma_{t-3D-appro}$ as shown in Figure 1-4.

At this step, it is necessary to remind that, in the current state of the art, ALE 2D numerical simulations do not provide an accurate estimation of the thermo-mechanical loadings. So, it is assumed that the shape of these loadings are relevant, but not their magnitudes. This weak point is compensated by the measurement of the experimental cutting force and penetration force that are compared to the numerical values of cutting force and penetration force (Figure 1-3). The ratio between measured and numerical values provides two compensation factors (GFY and GFZ) that enable to calibrate the magnitudes of thermo-mechanical loadings (Figure 1-5). The 3D thermo-mechanical loadings are now defined and calibrated: the 3D density of heat flux $\varphi_{th-3D-calibrated}$, normal stress $\sigma_{n-3D-calibrated}$ and tangential stress $\sigma_{t-3D-calibrated}$. More details are available in [5].

Figure 1-6 shows the final step consisting in applying the 3D loadings onto the machined surface. The 3D loadings are applied with a velocity equal to the cutting speed. It is mandatory to simulate several revolutions until reaching a steady state in term of residual stress state. At least five revolutions are necessary. These multiple simulations are performed thanks to the finite element SYSWELD software based on an implicit formulation. After the cooling phase, this model makes 3D residual stress prediction possible. This hybrid model (hybrid=num. model + exp. force meas.) for residual stress prediction presents advantages like the absence of highly distorted mesh, the possibility of 3D multi-revolution simulations and accurate mechanical equilibrium computation. Finally, residual stress state beneath the surface is extracted and analysed in the cutting direction and in the feed direction (Figure 1-6). The accuracy of this model has been validated in longitudinal finish turning of a martensitic stainless steel 15-5PH [5] and an austenitic stainless steel 316L [8].

This model has the potential to be applied with any kind of cutting tools, trajectories and cutting conditions. However, it has only been validated for cylindrical surfaces produced by longitudinal finish turning. So, the aim of this paper consists in investigating the ability of this model to predict residual stresses for a more complex trajectory: a fillet radius (Figure 2a) machined by finish turning.

2. Experimental results

The case study consists in finish turning of a R=5 mm fillet radius made of a martensitic stainless steel 15-5PH in its H1025 state. The operation starts with longitudinal turning operation (green zone in Figure 2a), then comes the machining of the concave surface (fillet radius), and finally the face turning (orange zone in Figure 2a) in which the tool is fed radially towards the external diameter. The cutting tool and the cutting conditions are similar to the ones used in [5]:

- Insert : DNMG150608 PM 4325 (Sandvik)
- Cutting speed, V_c = 120 m/min
- Feed, f = 0.2 mm/rev
- Depth of cut, a_p = 0.2 mm
- Cutting fluid = dry

Residual stresses were estimated by means of X-Ray diffraction with the same measuring conditions and set-up as described in [9]. Figure 2b and 2c plots the residual stress profiles in the cutting direction and in the feed direction

respectively for 2 areas: the cylindrical area (longitudinal turning) and the plane area (face turning).
The shapes of the profiles are typical in finish turning of the 15-5PH as shown by previous works of the authors [4,5,9,10]. The external surfaces exhibit tensile stresses, followed by a peak of compression. Finally, the profiles come back to the stress state in the bulk of the part. These curves reveal that the intensity of residual stresses is much higher for the longitudinal turning than for the face turning. The peak of compression is more intense, and the affected depth is also wider.
NB : it is possible to observe a small unusual variation of the residual stress curves within the first 5 to 10 µm. This phenomenon is probably due to microstructural variation, especially dynamic recrystallisation phenomena as shown by [11]. These local phenomena will not be investigated in this model.
At this step, it is not possible to explain why such difference of residual stress profiles are observed between longitudinal and face turning. It can be assumed that the two areas have been machined with different cutting conditions with respect to the variation of trajectory.

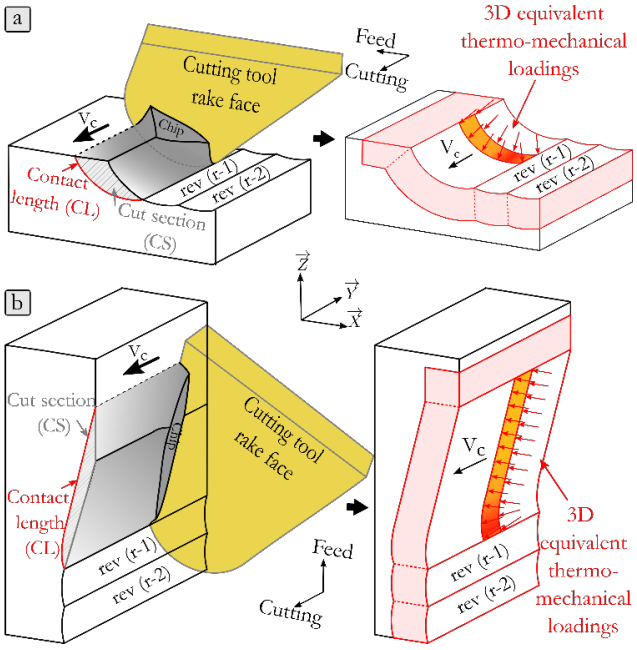

Fig. 3. Variation of the uncut section and of the model's geometry.

This is investigated by means of Figures 3 and 4. Figure 3 illustrates the two cutting configurations and Figure 4b plots the evolution of the area of the cut section CS and of the average uncut chip thickness h_m (defined in Figure 4a) during the machining of the part. They highlight that, in longitudinal and face turning, the cut section *CS* are similar as it corresponds to the equation f x a_p (= 0.2x0.2). However the average uncut chip thickness h_m is much thinner in face turning (0.01 ⇔ 0.06 mm) (Figures 3b and 4c and 4d). As a consequence, the contact length *CL* is much bigger for the face turning configuration (Figure 3b and 4c and 4d). So, even if the macroscopic cutting conditions programmed on the machine are similar (V_c, f, a_p), the cut section is short and thick in longitudinal turning (Figure 3a), whereas it is long and thin in face turning. This is a first element that may explain the variation of residual stress profiles revealed in Figure 2.
Moreover, the introduction of this paper has reminded that the model predicting residual stresses requires the measurement of cutting F_c and penetration F_p forces so as to calibrate the intensity of the thermo-mechanical loadings applied on the machined surface. So, forces have been monitored during the finish turning operation thanks to a Kistler dynamometer clamped on the turret of the CNC lathe. The evolutions of the three components are plotted in Figure 4b.

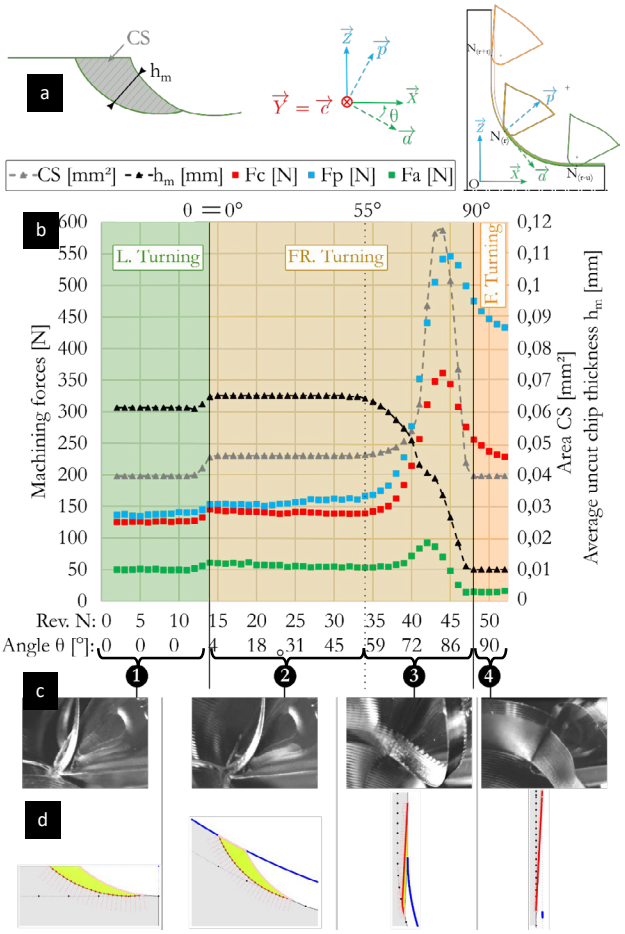

Fig. 4. Evolution of force components, uncut chip thickness and area when turning a fillet radius.

NB : The penetration force F_p changes its orientation during the turning of the fillet radius. During longitudinal turning F_p is parallel the Z axis, whereas, during face turning F_p is parallel to the X axis. So F_p has been computed from the two components of the Kistler dynamometer.
It can be observed that cutting F_c and penetration F_p forces are very similar in longitudinal turning, whereas they are very different in face turning. Especially the penetration force F_p is twice higher than the cutting force F_c in face turning.
So, the significant variation of the cut sections and of the forces between the longitudinal and face turning operations should be responsible for the significant variation of the residual stress state.

As far as the fillet radius is concerned, it was not possible to characterize the residual stress state as the DRX system was not able to reach properly the surface. However, the geometrical parameters are available for each position (each θ angle in Figure 2a) and the cutting forces have also been recorded. Figure 4 reveals that the cut section, the average chip thickness and the forces vary continuously in the fillet radius. It is shown that the area of the cut section is not constant and reaches a maximum value for an angle θ ~ 80°. This zone corresponds also to a significant increase of the cutting F_c and penetration F_p forces. Therefore, it can be assumed that the residual stress state should also vary continuously with the variation of the cut section and forces. The new model should be able to simulate the residual stress state for each position thanks to the collected input data. This will be the topic of the next section.

3. Numerical results

The model presented in Figure 1 and summarized in section 1 has been applied for some position (θ = 0-30-75-78-80-90°) along the fillet radius. The position θ=0° corresponds to the longitudinal turning configuration, whereas θ=90° corresponds to the face turning configuration. For each position, the cut section has been divided into several 2D elementary orthogonal sections $S_{(i)}$ having a local uncut chip thickness $h_{(i)}$ (Figure 1b). For each section $S_{(i)}$, a 2D numerical model (ABAQUS explicit with an ALE formulation – details in [5]) simulates the material removal as shown in Figure 1c. At this step, it is not necessary to launch all the simulations for each cut section. The simulations having similar uncut chip thickness $h_{(i)}$ can be shared among the various cut section. So, in practice, it is only necessary to simulate around 5 orthogonal cutting configurations in ABAQUS ($h_{(i)}$ = 0.01-0.02-0.035-0.05-0.06 mm). So, at this step of the model, the additional time required to simulate a fillet radius instead of a simple longitudinal operation, is very limited. This is a clear advantage of the model.

Based on these ABAQUS simulations, the thermo-mechanical loadings are extracted along the line called "extraction path". This provides the 2D density of heat flux $\varphi_{th-2D(i)}$, the normal stress $\sigma_{n-2D(i)}$ and the tangential stress $\sigma_{t-2D(i)}$ along the extraction path, applied to the workpiece (Figure 1d). By combining these 2D loadings on the effective machined surface (Figure 1e). As discussed previously, the surface differs significantly along the fillet radius. In the longitudinal cutting area, the surface is a cylinder that is generated by the edge radius of the insert (Figure 3a). On the contrary, in the face turning area, the surface has a small cylindrical zone and the wide majority is a flat surface generated by the main cutting edge (Figure 3b). In between, the surface is a mix between a cylinder and a plane.

For each surface, it becomes possible to model the 3D density of heat flux $\varphi_{th-3D-appro}$, normal stress $\sigma_{n-3D-appro}$ and tangential stress $\sigma_{t-3D-appro}$ as shown in Figure 1e. Then, the 3D thermo-mechanical loadings are calibrated thanks to the forces (Figure 4): the 3D density of heat flux $\varphi_{th-3D-calibrated}$, normal stress $\sigma_{n-3D-calibrated}$ and tangential stress $\sigma_{t-3D-calibrated}$. Then 3D loadings are applied on the surface (Figure 3a or 3b) with a velocity equal to the cutting speed (software SYSWELD implicit details in [5]). It is mandatory to simulate several revolutions until reaching a steady state in term of residual stress state. Finally, residual stress state beneath the surface is extracted and analyzed in the cutting direction and in the feed direction for each position (Figure 5a).

Several simulations for a large number of positions have been performed. But only a selection has been presented in the paper. Figure 5a illustrates the distribution of the residual stresses in the cutting direction for 6 angular positions from longitudinal turning at 0° to face turning at 90° (0-30-75-78-80-90°). Figure 5b and 5c plot the residual profiles in the feed and cutting direction respectively. It is clear that the residual stresses evolve continuously from one end of the fillet to the other.

NB : The sensitivity of the residual profiles is especially very high around the position θ between 75-80° where there is a strong gradient of chip thickness h_m and cutting section CS (Figure 4).

The most intense and deepest profiles are obtained for the shortest and thickest chips (area close to the longitudinal turning area), while the less intense stress profiles are obtained for the areas generating thin and long chips (face turning). Thus, the model enables to highlight the existence of a continuous variation of the residual stress state in relation to the variation of the tool-workpiece contact area, the corresponding local chip thickness and in relation to the variation of the cutting and penetration forces.

If we focus more specifically on the extremities: the case of longitudinal turning and face turning, Figure 2 plots the experimental and numerical profiles. It appears that the model, proposed by [5], provides a reasonable prediction of the evolution of the stress profiles. This allows to have a good confidence on the intermediate profiles which could not be measured.

4. Conclusions

This paper has investigated the possibility to predict residual stresses when finish turning a fillet radius on a shaft made of a martensitic stainless steel 15-5PH. A recently proposed model was available for longitudinal turning operations. This model is based on the application of 3D equivalent thermo-mechanical loadings on the machined surface. This model has been applied for a more complex configuration (fillet radius). It has been shown that the geometrical configuration (cut section, uncut chip thickness, …) and the forces vary all along the tool path. As a consequence, the thermo-mechanical loadings vary also continuously along the path. The accuracy of model has been validated for two configurations with a reasonable accuracy. So, it is reasonable to conclude on the ability of the model to predict the residual stress state over the fillet radius.

This work has highlighted that longitudinal turning leads to small and thick chips that are responsible to residual stress profiles with a deep affected depth and high magnitude. On the contrary, face turning leads to long and thin chips that are responsible for residual stress profiles with a slight affected depth and a smaller magnitude.

A perspective of the work consists in applying this model for other workmaterials and other complex geometries so as to evaluate its universality.

References

[1] Davim, J.P., 2008. Machining: fundamentals and recent advances. Springer Science & Business Media.

[2] Jawahir, I., Brinksmeier, E., M'Saoubi, R., Aspinwall, D., Outeiro, J., Meyer, D., Umbrello, D., Jayal, A., 2011. Surface integrity in material removal processes: Recent advances. CIRP annals 60, 603–626.

[3] Chomienne, V., Verdu, C., Rech, J., Valiorgue, F., 2013. Influence of surface integrity of 15-5ph on the fatigue life. Procedia Engineering 66, 274– 281.

[4] Dumas, M., Valiorgue, F., Van Robaeys, A., Rech, J., 2018. Interaction between a roughing and a finishing operation on the final surface integrity in turning. Procedia CIRP 71, 396–400.

[5] Dumas, M., Fabre, D., Valiorgue, F., Kermouche, G., Van Robaeys, A., Girinon, M., Brosse, A., Karaouni, H., Rech, J., 2021. 3d numerical modelling of turning-induced residual stresses–a two-scale approach based on equivalent thermo-mechanical loadings. Journal of Materials Processing Technology 297, 117274.

[6] Attanasio, A., Ceretti, E., Giardini, C., 2009. 3d FE modelling of superficial residual stresses in turning operations. Machining science and technology 13, 317-337.

[7] Salio, M., Berruti, T., De Poli, G., 2006. Prediction of residual stress distribution after turning in turbine disks. International Journal of Mechanical Sciences 48, 976-984.

[8] Aridhi, A., Dumas, M., Perard, T., Girinon, M., Brosse, A., Karaouni, K., Valiorgue, F., Rech, J., 2022. 3D Numerical modelling of turning-induced residual stresses in 316L stainless steel. Procedia CIRP 108,885-890.

[9] Mondelin, A., Valiorgue, F., Rech, J., Coret, M., Feulvarch, E., 2012. Hybrid model for the prediction of residual stresses induced by 15-5ph steel turning. International Journal of Mechanical Sciences 58, 69-85.

[10] Valiorgue, F., Rech, J., Hamdi, H., Gilles, P., Bergheau, J.M., 2012. 3d modeling of residual stresses induced in finish turning of an aisi304l stainless steel. International Journal of Machine Tools and Manufacture 53, 77–90.

[11] Mondelin, A., Rech, J., Feulvarch, E., Coret, M., 2014. Characterization of martensite-austenite transformation during finish turning of an AISI S15500 stainless steel, IJMMM, 15(1-2)101-121

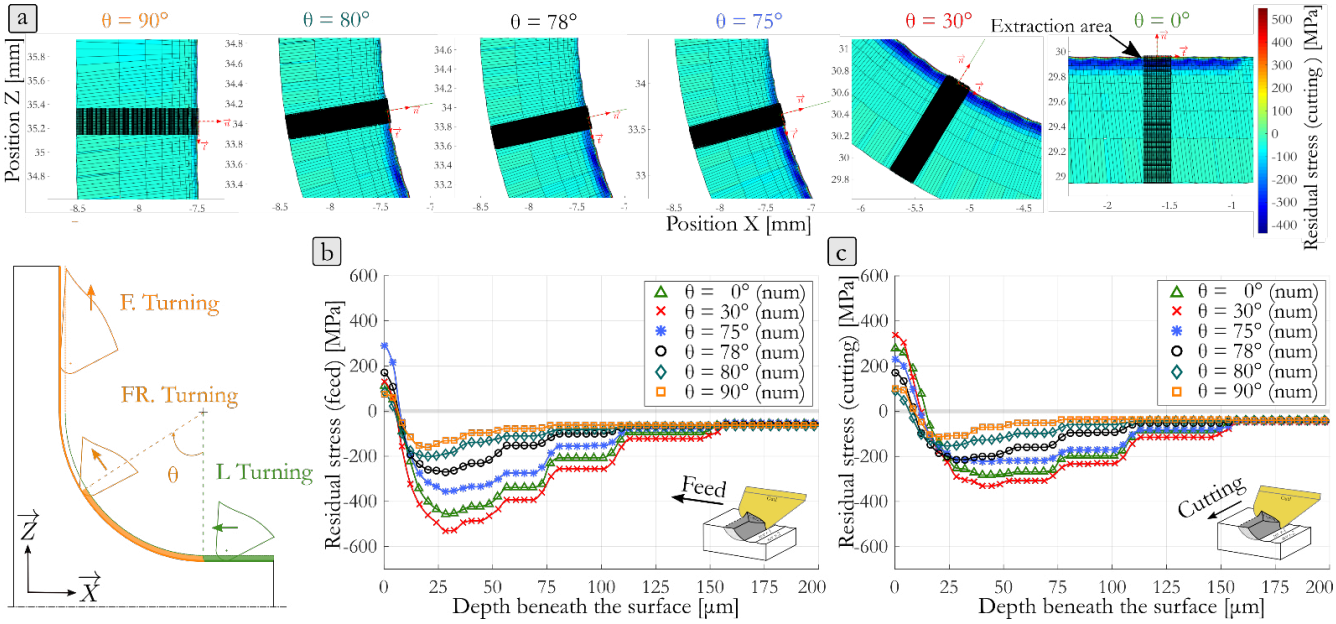

Fig. 5. Evolution of residual stresses induced by turning around a fillet radius